# Optical study of niobium disilicide polycrystalline films

M. Amiotti, A. Borghesi, and F. Marabelli
*Dipartimento di Fisica "A. Volta," Università degli Studi di Pavia, Via Bassi 6, I-27100 Pavia, Italy*

G. Guizzetti and F. Nava
*Dipartimento di Fisica, Università degli Studi di Modena, Via Campi 210/A, I-41100 Modena, Italy*
(Received 14 February 1991)

$NbSi_2$ polycrystalline films, coevaporated and thermally annealed, were subjected to chemical and structural characterization, and then studied by reflectance from 0.06 to 6 eV and ellipsometry from 1.4 to 5 eV. The dielectric functions, obtained from Kramers-Kronig analysis and directly from ellipsometry, are also presented. Low-frequency free-carrier response is discussed in terms of the Drude model; the high-frequency interband structures are interpreted on the basis of the calculated density of states and photoemission results. A comparison is made with the optical properties of isoelectronic $VSi_2$ and $TaSi_2$ polycrystalline films.

## I. INTRODUCTION

Severe demands upon high-temperature interconnect materials with resistivity lower than polysilicon are made in very-large-scale integration in order to lower the propagation delay. Refractory metal silicides have received a great deal of interest due to their low resistivity, oxidation resistance, and compatibility with metal-oxide-semiconductor (MOS) processes.[1] $NbSi_2$-gate MOS capacitors were fabricated on both $n$-type and $p$-type Si substrates.[2] $NbSi_2$ is overall compatible with standard MOS processing, except that buffered HF solution etches it slowly.[2,3] The possibility of growing epitaxially niobium silicide on Si finds potential application in the fabrication of electronic devices employing buried metal layers.[4]

The structural properties and the crystallization kinetics of $NbSi_2$ have already been investigated by x-ray diffraction (XRD), Rutherford backscattering spectroscopy (RBS), transmission electron microscopy (TEM), Auger electron spectroscopy (AES), and secondary-ion mass spectrometry.[2,5-7] Electrical-resistivity measurements[2,5-7] (one connected with Hall measurements[6]) have been used to determine transport parameters. The niobium silicide formation induced by Ar (Ref. 9) and Ge or As (Ref. 10) ion implantation on evaporated-Nb-on-Si systems has been studied extensively. Chow, Hamzeh, and Steckl[11] have demonstrated that after thermal annealing of sputtered niobium silicide on $SiO_2$ both metal and silicon oxides coexist on the top of the silicide. The epitaxial growth of $NbSi_2$ on Si(111) has been analyzed by TEM and AES.[4] The general trend of bonding in a variety of transition-metal disilicides including $NbSi_2$ has been studied by angle-integrated synchrotron radiation photoemission.[12] More recently a systematic experimental and theoretical study of the electronic structure of $NbSi_2$ and of isoelectronic $VSi_2$ and $TaSi_2$ has been reported,[13,14] in which x-ray photoemission (XPS) and ultraviolet photoemission spectroscopy (UPS) as well as bremsstrahlung isochromat spectroscopy (BIS) have been used as experimental techniques, and the results have been interpreted by calculating the density of states (DOS) and the matrix elements. XPS and x-ray emission spectroscopy on amorphous $Nb_{1-x}Si_x$ and hexagonal $NbSi_2$ were combined to study the role of the silicon $s$ and $p$ and the niobium $d$ electrons in bonding and band structure of the Nb-Si alloys.[15,16] Lastly, XPS, UPS, and AES studies showed that the Nb/Si(111) interface is very reactive.[17]

In this paper we report the reflectivity spectra of $NbSi_2$ from the far infrared to the vacuum ultraviolet and the dielectric functions obtained both by Kramers-Kronig transformations and directly measured by ellipsometry. To our knowledge this is the first study on the optical spectra, because the only previous report[18] concerned the optical constants at a fixed wavelength ($\lambda$=632.8 nm). This work completes the optical investigation of the silicides of group-VB metals (i.e., V and Ta),[19,20] with which a comparison is made.

## II. EXPERIMENTAL PROCEDURE AND RESULTS

Alloy films of composition $NbSi_{2.8}$ were coevaporated on thermally oxidized (~8000 Å) $SiO_2$ silicon wafers through a metallic mask to produce Van der Pauw patterns, each 1 $cm^2$ of area, for an accurate determination of the absolute value of resistivity and Hall voltage. A dual electron gun system in a vacuum chamber, with residual pressure lower than $10^{-7}$ Torr, was used for deposition. The deposition was carried out at room temperature with deposition rates of 5 Å/s for niobium and 10 Å/s for silicon. Particular care was taken in the specimen preparation in order to reduce the contamination by impurities (mainly O and C). The samples were annealed at 900 °C for 30 min in a quartz tube furnace with a flow of purified He gas. Furthermore, caution was taken to reduce the intake of impurities during the furnace heat treatments. The details of both processes have been described elsewhere.[20,21]

 ©1991 The American Physical Society

Several structural and compositional techniques were used to characterize these films.[7] RBS with a 2-MeV $^4He^+$ ion beam was used for depth compositional analysis and for determining the film thickness. A stoichiometric ratio of 1 to 2.8 was deduced for the as-deposited thin film. The annealing at 900 °C for 30 min promotes a nonuniform-in-depth segregation of the silicon, towards the inner interface and the stoichiometry ratio becomes 1 to 2.3. A heat treatment for longer times (5 h) does not modify the shape of RBS spectra and we can assume that the excess Si, upon the crystallization of $NbSi_2$, is still present as a mixture in the film. The thickness of annealed $NbSi_2$ was typically 1000 Å.

Crystalline phases and microstructures present in the films were identified by XRD with Bragg-Brentano geometry, by transmission electron diffraction and TEM. The as-deposited films were amorphous, while the annealed ones were fully crystallized, consisting of 800–1500–Å grains of $NbSi_2$ hexagonal phase. No evidence of niobium oxide compounds was found.

Surface morphology for both the as-deposited and fully annealed thin films was examined by scanning electron microscopy: the surfaces of as-deposited thin films were extremely smooth and remained very smooth after heat treatment.

Chemical elements and their relative concentration profiles were measured by AES combined with $Ar^+$ sputtering. In agreement with the RBS results, the $NbSi_2/SiO_2$ interface is characterized by a higher content of silicon in the annealed than in the as-deposited samples. Moreover, the oxygen peak detected inside the thin film is of the same order of magnitude of the noise, so the bulk of the $NbSi_2$ thin film can be regarded to be relatively free of the oxygen contamination. Carbon contamination has never been detected.

Finally, as far as the electrical properties are concerned, the temperature dependence of the resistivity shows a typical metallic behavior and its interpretation is reported in Ref. 7. At room temperature a value of 73 $\mu\Omega$ cm has been measured for the resistivity, while the sign of the Hall voltage indicates that the electrons are the dominant charge carriers.

Reflectance ($R$) measurements at near-normal incidence and at room temperature were performed in the 0.5–6 eV photon energy range, using an Al mirror covered with $MgF_2$ film as reference, by a Perkin Elmer 330 automatic spectrophotometer, with an accuracy of 0.5%. In the 0.06–0.6-eV range, instead, the reflectance was measured by a Fourier transform spectrometer Bruker IFS 113v, using an Au mirror as reference. In the overlapping spectral range, the $R$ values from the two spectrometers agree within the limits of experimental uncertainty. In the range from 1.4 to 5 eV the dielectric functions of the thin films were obtained by a spectroscopic ellipsometer SOPRA ES4G.

$R$ derived from ellipsometry is generally higher in the overlapping region than that directly measured by spectrophotometry (Fig. 1), but the structures are exactly localized at the same energy. As in other silicides[22–24] both $R$ and the dielectric function are expected to be influenced, mostly in the uv region, by macroscopic surface roughness causing light loss by scattering. This lowers the measured $R$, but not the ellipsometric results which do not require absolute intensity measurements.

Transmittance ($T$) has been measured in the spectral range between 0.5 and 1.3 eV, where the multilayer system $NbSi_2$-$SiO_2$-Si (substrate) is transparent.

The $R$ (and $T$) spectrum presents interference fringes in the region from 0.4 to 2 eV. In order to obtain the refraction index ($n$) and the extinction coefficient ($k$) of $NbSi_2$ in this zone we fitted the spectra with the expressions of $R$ and $T$ for a multilayer.[25] The thickness of each layer was known from RBS and the optical functions of amorphous $SiO_2$ and crystalline Si were taken from the literature.[26] The $n$ and $k$ values from the fit where used to derive the absolute reflectivity $R_a$ (Fig. 1).

We tried also to invert $R$ and $T$ expressions to obtain $n$ and $k$, but it was useless because the system is not ideal with plane-parallel and sharp interfaces, so in some points nonphysical or no solutions were obtained for $n$ and $k$. For the same reasons the fit does not reproduce exactly the experimental curves, but it represents the best choice for the optical parameters of $NbSi_2$ in order to describe the system with a simple model without any external parameter (roughness, interlayer transition region, etc.). About the goodness of the fit, we observe that all the interference fringes are well reproduced at the correct wavelengths both in $R$ and $T$ spectra. The intensities generally agree within the limit of experimental uncertainty, except at the minima of interference fringes in the reflectance due, probably, to the deviation from

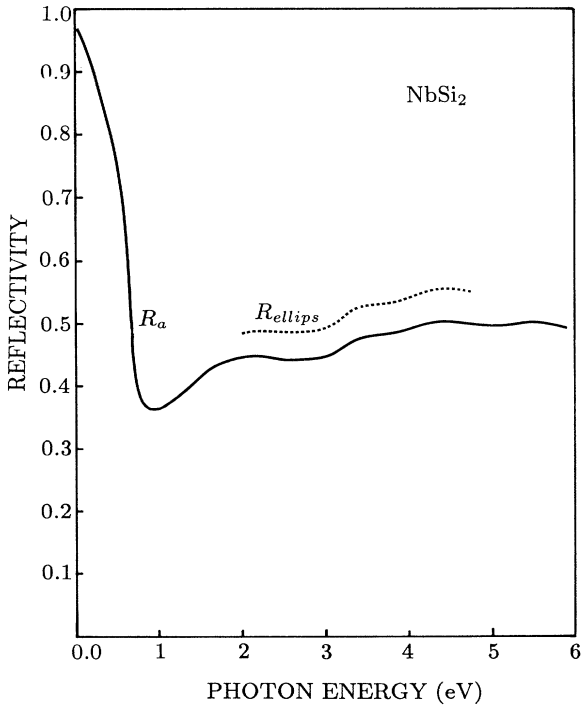


FIG. 1. Room-temperature absolute reflectivity ($R_a$) of $NbSi_2$. The spectrum derived from ellipsometric measurements ($R_{ellips}$) is also reported.

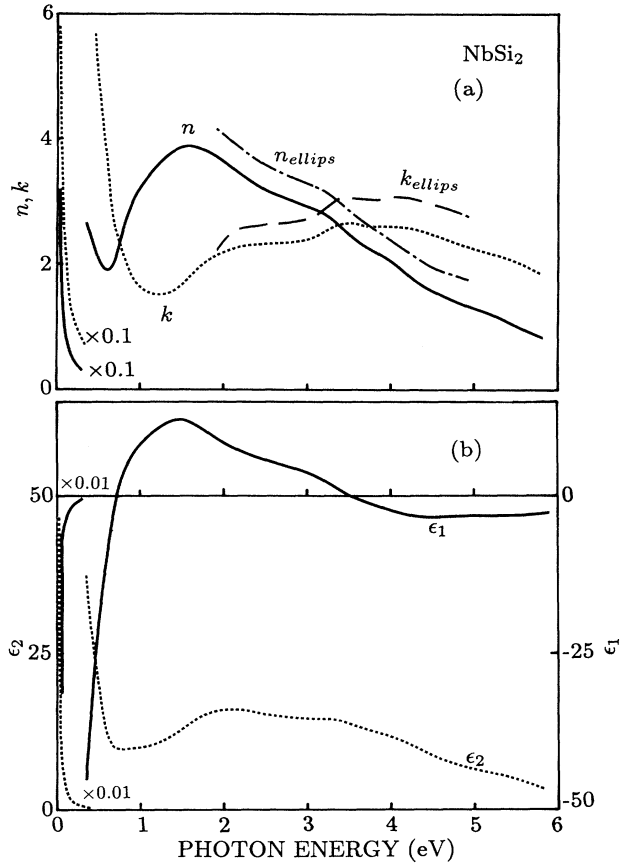


FIG. 2. (a) Refractive index ($n$) and extinction coefficient ($k$) of $NbSi_2$ obtained by Kramers-Kronig analysis, compared with those measured by ellipsometry ($n_{ellips}$ and $k_{ellips}$). (b) Real ($\epsilon_1$) and imaginary ($\epsilon_2$) parts of the dielectric function of $NbSi_2$.

ideal conditions at the interfaces.

In the fit procedure we always checked the consistency of $n$ and $k$ through the Kramers-Kronig (KK) causality relations. This provided us also with the complex dielectric function $\tilde{\epsilon}(\omega) = \epsilon_1(\omega) + i\epsilon_2(\omega)$ and the complex refraction index $\tilde{n}(\omega) = n(\omega) + ik(\omega)$ (Fig. 2) outside the ellipsometric range, completing the description of the optical properties of $NbSi_2$. In the KK procedure we extrapolated the $R_a$ spectrum of Fig. 1 beyond the highest experimental energy $\omega_0$ with a tail $R_a(\omega) = R_a(\omega_0)\ (\omega_0/\omega)^s$. The $s$ value was determined in order that the calculated $n$ and $k$ showed the same shape of those directly measured by ellipsometry. We obtained $s \approx 2$ , which is very close to the values found for other disilicides.[19,24] The values of $\epsilon_2$ at low frequencies were consistent with the measured dc conductivity.[7]

## III. DISCUSSION

The knowledge of the electronic band structure, the related joint density of states (JDOS), and oscillator strength is indispensable for an accurate interpretation of the optical spectra. Because no JDOS has been calculated for Nb silicides, we will qualitatively discuss the response of $NbSi_2$ and some trends in the spectra of isoelectronics V, Nb, and Ta disilicides on the basis of DOS and the chemical bonding properties. This series of refractory metal (column VB) disilicides is particularly suitable for a direct comparison, because they are not only isoelectronic, but also crystallize in the same structure of $CrSi_2$ (C40). Such a comparison has already been performed[13,14] between experimental XPS and BIS spectra and theoretical spectra, obtained from calculated DOS with explicit inclusion of the appropriate solid-state matrix elements. The good agreement between experiments and theory has provided a detailed and reliable analysis of the electronic structure of these silicides, of which we recall the main features.

The underlying physical principle in the chemical bonding of all transition-metal silicides is the competition between the strong metal $d$–metal $d$ interaction and the formation of metal $d$–Si $p$ bonds.[27] The hybridization $d$–$p$ produces bonding and antibonding states separated by a nonbonding (purely $d$) region or by a low density of Si $p$ states region (often called "quasigap") straddling $E_F$. In the case of refractory metal disilicides the splitting between bonding and antibonding states increases going from V to Ta. This is due to an increased overlap of the metal $d$ and Si $p$ orbitals, consequent to the larger spatial extension going from $3d$ to $5d$ wave functions. However, contrary to other silicides or earlier schemes, in the quasigap the states do not present pure metal $d$ character, but always some mixing with Si (mainly $p$) states.[14] Moreover, the band originating from Si $s$ orbitals participates in the bonding interaction, although its main part is well separated from the main $p$–$d$ hybrid bands. Specifically, in the $NbSi_2$ the DOS presents valence bands mainly with Si $s$ character from $-7$ to $-12$ eV (relative to $E_F$), followed by the bonding Nb $d$–Si $p$ states centered around $-2.5$ eV and their antibonding counterparts around 2–4 eV.

On the basis of this information we analyze the optical response of $NbSi_2$ by distinguishing two different regions, typical of a metal: the intraband, due to the free electrons, and the interband regions. At low energy the $R_a$ spectrum displays a high shoulder, followed by a sharp cutoff with a minimum near 1 eV, roughly corresponding to the energy of the free-carrier hybrid resonance, screened by the interband transitions. These latter determine the second region where $R_a$ increases again, showing a shoulder at 1.7 eV and peaks at 2.1, 3.3, 4.5, 5.6 eV.

A similar behavior is displayed by the reflectivities of both Nb pure metal[28] and V and Ta disilicides.[19,20] However in Nb the plasma minimum falls at ~2.2 eV, while in $VSi_2$ it falls at ~0.8 eV and in $TaSi_2$ at ~1.1 eV. These differences are well understood on the basis of the aforementioned DOS structure, remembering that the cutoff in $R$ is determined by the arising of interband transitions. In pure Nb metal the strong $d$-$d$ bonding-antibonding interaction splits the $d$ bands into two groups of states, straddling $E_F$. Therefore the low-energy interband transitions occur between occupied $d$-like bands and unoccupied $p$-like bands. The augmented Nb-Nb distance in the disilicide leads to a drastic reduction of the $d$-$d$ interaction and of the quasigap between bonding and antibond-

ing $d$-$p$ hybrid bands, so the first interband transitions occur at lower energies in $NbSi_2$ than in Nb metal. The shift towards higher energies of the plasma minimum in $R_a$ going from V to Ta disilicides is directly connected to the corresponding broadening of the quasigap. This trend is displayed also by the low-energy interband structures, which are located near 1.0 and 1.7 eV in $VSi_2$, near 1.7 and 2.1 eV in $NbSi_2$, and near 1.4 and 2.4 eV in $TaSi_2$.

Even in $NbSi_2$, as in V and Ta disilicides, the free-carrier far-infrared response is well fit by the Drude dielectric function:

$$\tilde{\epsilon}(\omega) = \epsilon_1 + i\epsilon_2 = \epsilon_\infty - \frac{\omega_p^2\tau^2}{1+\omega^2\tau^2} + i\frac{\omega_p^2\tau}{\omega(1+\omega^2\tau^2)}, \quad (1)$$

where $\epsilon_\infty$ is the high-frequency interband contribution, $\omega_p$ and $\tau$ the plasma frequency and the relaxation time of the free carriers. In fact, the plots of $1/\epsilon_1$ and of $\omega\epsilon_2$ vs $\omega^2$ show linearity, for $\omega < 0.2$ eV, according to Eq. (1). These plots give $\omega_p \simeq 2.3$ eV and $\tau \simeq 1.2 \times 10^{-14}$ sec, and an optical resistivity at zero frequency $\rho_{\rm opt} = 4\pi/\omega_p^2\tau \simeq 68\ \mu\Omega\,$cm which compares well with the dc resistivity $\rho_{\rm dc} = 73\ \mu\Omega\,$cm. Nevertheless we note that, even if its order of magnitude is correct, the value of $\omega_p$ is not intermediate, as one would expect, between those of $VSi_2$ (2.75 eV) and $TaSi_2$ (2.6 eV), which have been obtained optically in the same way.[19,20] At the same time the value of $\tau$ seems to be too high. These small discrepancies are due to the fact that the investigated $NbSi_2$ samples were much thinner than $VSi_2$ and $TaSi_2$ samples, so that also in the far-infrared we observe interference effects. Even if these effects are accounted for, the resulting absolute reflectivity is less accurate, giving a higher uncertainty in $\tilde{\epsilon}$. If instead we derive $\omega_p$ from the energy value $\omega = 0.7$ eV, where $\epsilon_1 = 0$, which is less sensitive to the value of $R_a$, and take into account that $\epsilon_\infty \simeq 15$, we obtain $\omega_p \simeq 2.8$ eV, in good agreement with the previously reported values. From the $\omega_p$ value we can derive the electron velocity at the Fermi surface through the relation[29]

$$\rho_{\rm sat} = 4.95 \times 10^{-4}\frac{\langle v_F\rangle}{\langle\omega_p^2\rangle a}, \quad (2)$$

where $\rho_{\rm sat}$=345 $\mu\Omega\,$cm represents the limiting value in the resistivity saturation phenomenon, described in Ref. 7. Here $a$ is the length, of the order of interatomic distance, somewhere between the lattice constant $a_0$ and the nearest-neighbor distance $a_n$ ($a_0 \le a \le a_n$), which can be defined by means of the minimum time between collisions $\tau$ as $\tau = a/\langle v_F\rangle$. We do not know the precise value of $a$ to be used in Eq. (2), so we assumed $a \approx a_n$ for an evaluation of $\langle v_F\rangle$ in the first approximation. With $a$ = 3 Å and $\omega_p$ between 2.3 and 2.8 eV, the value of $\langle v_F\rangle$ is between $1.2\times10^7$ and $1.6\times10^7$ cm/s, which may be compared with the value of $0.9$–$2.9\times10^7$ cm/s found in other disilicides.[30–32]

## ACKNOWLEDGMENTS

This work was partially supported by Progetto Finalizzato "Materiali e Dispositivi per Elettronica a Stato Solido" and by Gruppo Nazionale Struttura della Materia del Consiglio Nazionale delle Ricerche, Italy.

[1] S. P. Murarka, *Silicides for VLSI Applications* (Academic, New York, 1983).
[2] C. D. Rude, T. P. Chow, and A. Steckl, J. Appl. Phys. **53**, 5703 (1982).
[3] T. P. Chow and F. G. Fanelli, J. Electrochem. Soc. **132**, 1969 (1985).
[4] C. S. Chang, C. W. Nieh, J. J. Chu, and L. J. Chen, Thin Solid Films **161**, 263 (1988).
[5] J. E. E. Baglin, F. M. d'Heurle, W. N. Hammer, and S. Petersson, Nucl. Instrum. Methods **168**, 491 (1980).
[6] W. Guoying, Z. Goubing, W. Y. Yuan, X. Wei, L. Y. Hong, C. G. Hopkins, and M. D. Strathman, J. Vac. Sci. Technol. B **3**, 1703 (1985).
[7] F. Nava, P. A. Psaras, H. Takai, K. N. Tu, S. Valeri, and O. Bisi, J. Mater. Res. **1**, 327 (1986).
[8] T. P. Chow, W. J. Lu, A. J. Steckl, and B. J. Baliga, J. Electrochem. Soc. **133**, 175 (1986).
[9] T. Kanayama, H. Tanoue, and T. Tsurushima, Appl. Phys. Lett. **35**, 221 (1979).
[10] F. M. d' Heurle, C. S. Petersson, and M. Y. Tsai, J. Appl. Phys. **53**, 8765 (1982).
[11] T. P. Chow, K. Hamzeh, and A. J. Steckl, J. Appl. Phys. **54**, 2716 (1983).
[12] J. H. Weaver, A. Franciosi, and V. L. Moruzzi, Phys. Rev. B **29**, 3293 (1984).
[13] W. Speier, E. v. Leuken, J. C. Fuggle, D. D. Sarma, L. Kumar, B. Dauth, and K. H. J. Buschow, Phys. Rev. B **39**, 6008 (1989).
[14] W. Speier, L. Kumar, D. D. Sarma, R. A. de Groot, and J. C. Fuggle, J. Phys. Condens. Matter **1**, 9117 (1989).
[15] W. Zahorowski, A. Simunek, G. Wiech, K. Söldner, R. Knauf, and G. Saemann-Ischenko, J. Phys. C **9**, 1025 (1987).
[16] E. Zöpf, Thesis, Universität München, 1972.
[17] M. Azizan, T. A. Nguyen, R. C. Cinti, G. Chauvet, and R. Baptist, Solid State Commun. **54**, 895 (1985).
[18] P. A. Heimann, S. P. Murarka, and J. Rosario, Mater. Lett. **2**, 31 (1983).
[19] A. Borghesi, L. Nosenzo, A. Piaggi, G. Guizzetti, C. Nobili, and G. Ottaviani, Phys. Rev. B **38**, 10 937 (1988).
[20] A. Borghesi, A. Piaggi, G. Guizzetti, F. Nava, and M. Bacchetta, Phys. Rev. B **40**, 3249 (1989).
[21] F. Nava, K. N. Tu, E. Mazzega, M. Michelini, and G. Queirolo, J. Appl. Phys. **61**, 1085 (1986).
[22] A. Humbert and A. Cros, J. Phys. (Paris) Lett. **44**, L-929 (1983).
[23] F. Ferrieu, C. Viguier, A. Cros, A. Humbert, O. Thomas, R. Madar, and J. P. Senateur, Solid State Commun. **62**, 455 (1987).
[24] A. Borghesi, A. Piaggi, G. Guizzetti, L. Lévy, M. Tanaka,

and H. Fukutani, Phys. Rev. B **40**, 1611 (1989).
[25] O. S. Heavens, *Optical Properties of Thin Solid Films* (Butherworths, London, 1955).
[26] *Handbook of Optical Constants of Solids,* edited by E.D. Palik (Academic, Orlando, 1985).
[27] C. Calandra, O. Bisi, and G. Ottaviani, Surf. Sci. Rep. **4**, 271 (1985).
[28] J. H. Weaver, C. Krafka, D. W. Lynch, and E. E. Koch, *Physics Data: Optical Properties of Metals* (Fachinformations-zentrum, Karlsruhe, 1981).
[29] P. B. Allen, Phys. Rev. B **17**, 3725 (1978).
[30] I. Engstrom and B. Lonnberg, J. Appl. Phys. **63**, 4476 (1988).
[31] M. T. Huang, T. L. Martin, U. Malhotra, and J. E. Mahan, J. Vac. Sci. Technol. B **3**, 836 (1985).
[32] A. Borghesi, F. Marabelli, G. Guizzetti, M. Michelini, and F. Nava, J. Appl. Phys. **69**, 7645 (1991).